

Filip WASILCZUK*, Michał WASILCZUK**, Michał WODTKE***

PROSPECTS OF DECREASING POWER LOSSES IN A HYDROSTATIC THRUST BEARING

MOŻLIWOŚĆ ZMNIEJSZENIA STRAT TARCIA W HYDROSTATYCZNYM ŁOŻYSKU WZDŁUŻNYM

Key words: hydrostatic thrust bearing, friction losses, hydrodynamic thrust bearing.

Abstract In numerous machines, axial load is carried by tilting pad thrust bearings known since the beginning of 20th century. These bearings are commonly bath lubricated, which is simple, does not require any additional pumps, and, due to this, such systems are highly reliable. In a contemporary technology, however, minimization of friction losses became an important goal of machinery improvement. Calculations based on elementary rules of fluid dynamics show that shearing losses in a specially designed hydrostatic bearing can be considerably smaller than the losses in a tilting pad hydrodynamic bearing. The aim of the research described in this paper was to check if the preliminary results can also be confirmed with the use of more advanced CFD calculations.

Słowa kluczowe: hydrostatyczne łożysko wzdluzne, straty tarcia, hydrodynamiczne łożysko wzdluzne.

Streszczenie W wielu maszynach przenoszenie obciążeń osiowych umożliwiają znane od ponad 100 lat hydrodynamiczne łożyska wzdluzne z wahlowymi segmentami. Smarowanie tych łożysk bardzo często jest smarowaniem zanurzeniowym, niewymagającym zastosowania dodatkowych pomp, co jest zaletą z punktu widzenia niezawodności. We współczesnej technice ograniczanie strat tarcia stało się istotnym kierunkiem doskonalenia konstrukcji maszyn. Obliczenia przeprowadzone w oparciu o podstawowe prawa mechaniki płynów wskazują, że w specjalnie zaprojektowanym łożysku hydrostatycznym można uzyskać znaczące ograniczenia strat tarcia w porównaniu do łożyska hydrodynamicznego. Obiecujące wyniki skłoniły autorów do przeprowadzenia dokładniejszych obliczeń strat tarcia w łożysku hydrostatycznym za pomocą CFD (Obliczeniowej Dynamiki Płynów). Wyniki tych obliczeń zostały w artykule porównane do znanych z literatury danych dotyczących strat w hydrodynamicznych łożyskach wzdluznych z wahlowymi klockami.

INTRODUCTION

Tilting pad hydrodynamic bearings used in vertical shaft hydrogenerators are usually designed with hydrostatic jacking recesses and high pressure systems activated only in the periods of start-ups and shutdowns. The hydrostatic pockets machined in the faces of the pads are rather small and shallow, in order not to disturb the generation of the hydrodynamic pressure [L. 1]. Sometimes permanent hydrostatic operation is considered as a solution to the problems in thrust bearing operation [L. 2]. Permanent operation of tilting pad thrust bearings in hybrid (hydrostatic and hydrodynamic) mode was tested in pump turbines of

one of the Polish power plants showing considerably lower temperatures [L. 3]. Such an operation of a thrust bearing was also analysed theoretically by Ettles et al. [L. 4], who showed thicker films and lower temperature in a bearing with hybrid operation. Further analysis of Ettles results presented in [L. 5] showed that, because of lower temperature and higher oil viscosity, a bearing in hybrid operation had higher friction losses. A possible reason is that a hydrodynamic bearing used as a hybrid bearing is far from optimum from the point of view of minimizing losses. A hydrostatic bearing with minimum energy consumption should have a larger pocket. According to a basic theory [L. 6], in a stationary hydrostatic pad, the size of the pocket should be 60%

* Institute of Fluid – Flow Machinery Polish Academy of Sciences, ul. Fiszerka 14, 80-231 Gdańsk, Poland; Doctoral Studies, Faculty of Mechanical Engineering, Gdańsk University of Technology, ul. Narutowicza 11/12, 80-233 Gdańsk, Poland, e-mail: filip.wasilczuk@imp.gda.pl.

** Gdańsk University of Technology, Faculty of Mechanical Engineering, ul. Narutowicza 11/12, 80-233 Gdańsk, Polska, e-mail: mwasilcz@pg.gda.pl.

*** Gdańsk University of Technology, Faculty of Mechanical Engineering, ul. Narutowicza 11/12, 80-233 Gdańsk, Poland, e-mail: mwodtke@pg.gda.pl.

of the pad width. Such a bearing is best in terms of energy consumption including both components – obtaining high pressure and generating required oil flow. A relatively small area outside the pocket is a benefit from the point of view of friction losses, because the shearing of a thin fluid film occurs only in this area, while the shearing gradient in the thick film area of the pocket is much smaller and the areas outside the pocket are wide enough to decrease the oil flow, thus decreasing the power consumption for pumping. Basic calculations carried out for such a hydrostatic (hybrid) bearing are applied in the machines of Porąbka Żar power plant [L. 5] with the following assumptions: OD = 1.3 m, ID = 0.85 m, rotational speed 600 rpm, bearing axial load 2.25 MN, lubricating oil ISO VG-46 at constant temperature of 60°C, and a film thickness of 40 µm (at present, according to measurements [L. 7], the thickness in hydrodynamic regime hardly exceeds 20 µm). The calculations were performed assuming that the bearing will consist of 10 pads. In such a bearing, the necessary oil flow is 42.7 l/min, the power consumption for pumping is only 7.3 kW, and the total loss of approximately 125 kW, including pumping, is about half of the present losses in the hydrodynamic bearing. These results illustrate the fact that a substantial decrease of friction loss, due to a thicker film (in which shearing gradient is decreased) and a smaller thin film area can be obtained at a relatively low cost of energy used for pumping. Such encouraging results were the incentive to perform a further, more advanced study of potential benefits in friction losses. The first stage of this study, a theoretical comparison of losses in a hybrid thrust bearing and a tilting pad hydrodynamic bearing, based on numerical calculations is presented in this paper.

GOAL OF THE ANALYSIS

The goal of the analysis was to compare the existing numerical calculation results for a hydrodynamic bearing with the results of the simulation on a hydrostatic bearing in the same operating conditions. In the analysis, it was decided to use the same bearing diameters, load, rotational speed, average film thickness, and the same oil type supplied at the same temperature. Comparison of bearing losses obtained in both cases and their structure will show whether using hydrostatic instead of hydrodynamic bearings is feasible in terms of energy saving.

CALCULATION/MODELS

Geometry and calculation models description

Two separate CFD bearings models, one for hydrodynamic mode and the other for hydrostatic (hybrid) mode of bearing operation, were developed and

applied. Both bearings have the same inner and outer diameters, as well as the same number of pads for proper comparison. However, due to the principle of operation, the distance between the pads has to be larger for the hydrodynamic bearing; thus, the angular dimensions of the pads (and therefore the pad sliding areas) differ slightly. It was assumed that, in the case of hydrostatic bearing, deformations of the pad and collar would not be considered, and the bearing is operating at constant (assumed) film thickness. In the case of hydrodynamic bearing thermo-elastic deformations of the pad and collar (TEHD model) were taken into account. It was possible due to expanding hydrodynamic bearing analysis and the application of the FSI method. Both bearing model dimensions are presented in **Table 1**.

Table 1. Geometric parameters of the investigated bearings
Tabela 1. Parametry geometryczne badanych łożysk

	Hydrostatic	Hydrodynamic
Inner diameter [mm]	90	
Outer diameter [mm]	180	
No. of sectors/pads [-]	8	
Sector/pad angle [°]	45	38
Sector/pad sliding area [mm ²]	2250.6	2014.5

The hydrodynamic bearing model is a comprehensive FSI model with both fluid and solid parts modelled. It was devised for theoretical studies of thrust bearings carried out concurrently to experimental research at the test stand at Gdansk University of Technology [L. 8]. The hydrostatic bearing model was prepared for the purpose of comparison between hydrostatic and hydrodynamic bearings. Therefore, the depth of physical models necessary to fulfil the goal for which the models were created is different.

However, the key features of both models were kept the same in order to make the comparison meaningful. Both bearings have the same inner and outer radii as well as the same number of sections. The film thickness is variable in the hydrodynamic bearing; thus, it was impossible to have it identical in both cases. For this reason, in the hydrostatic bearing model, the film thickness was assumed as an average of the corresponding film thickness obtained in the calculations of the hydrodynamic bearing (30.05 µm for 2000rpm and 31.4 µm for 4000rpm). The load for both models was the same – 48.3 kN (per 8 segments) and the solution was obtained for two collar rotational speeds – 2000 and 4000 rpm. Finally, both bearings used ISO-VG 32 oil for CFD calculations. Its parameters are presented in **Table 2**. Oil flow is assumed to be incompressible, one-phase with no cavitation. Oil viscosity varies exponentially with temperature, based on experimental measurements.

Table 2. Parameters of ISO-VG 32 oil

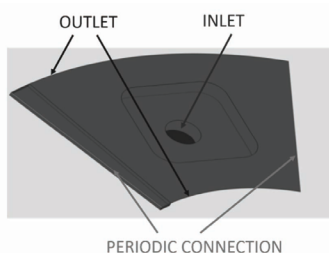
Tabela 2. Parametry oleju ISO-VG 32

Parameter	Unit	Value
Density ρ	[kg/m ³]	856
Specific heat c	[J/kg K]	2113.5
Viscosity at 40°C η_{40}	[Pa s]	27.32 x 10 ⁻³
Viscosity at 100°C η_{100}	[Pa s]	5 x 10 ⁻³

Boundary conditions

Hydrostatic bearing numerical solution was obtained using ANSYS/Fluent commercial solver using RANS approach with $k - \omega$ SST [L. 9] turbulence model. A structured mesh of 1.4 million elements was used.

Figure 1 presents the boundary conditions used in the model. At the inlet, constant static pressure was set in addition to oil temperature and turbulence parameters (**Table 3**). The outlet was situated at the inner and outer radii of the film gap with atmospheric conditions. The collar has been assigned appropriate rotational velocity according to the case. Both the collar and the pad walls were adiabatic walls, which is not entirely accurate, but gives more conservative results when it comes to the film temperatures and loads carried. In order to reduce the computation cost, the model features just one of eight pads; thus, the rotational periodicity boundary conditions were set.

**Fig. 1. Hydrostatic bearing boundary conditions schematics**

Rys. 1. Schemat warunków brzegowych w łożysku hydrostatycznym

Hydrodynamic bearing calculations were carried out using the Fluid-Structure Interaction (FSI) method, which allows for simultaneous analysis of the interacting oil flow and structural parts of the bearing. The load transfer between the oil flow and the structural bearing parts take place on the FSI surfaces, which are defined on the pad walls and the sliding and cylindrical surface of the collar. The analysis includes (TEHD bearing calculations): the oil flow in the gap and around the pad,

Table 3. Inlet boundary conditions for hydrostatic bearing model

Tabela 3. Warunki brzegowe na wlocie do łożyska hydrostatycznego

Boundary condition	Unit	Value
Inlet pressure	[MPa]	6.1-6.3
Inlet temperature	[°C]	40
Inlet k	[m ² /s ²]	0.00184
Inlet ω	[1/s]	2.46

heat flow, pad and collar thermoelastic deformation, and pad tilting. The applied computational model contained about 200 000 nodes in the fluid part and about 26 000 nodes in the solid part. A detailed description of the model can be found in [L. 10].

RESULTS

Main operational parameters

As mentioned before, the aim of this paper is to study the operation of hydrostatic and hydrodynamic bearings at similar operating conditions and assess their safety of operation and finally to compare the losses in each bearing type.

The main operational characteristics of the bearings are shown in the following figures. Both sets of graphs are presented to compare the distribution of pressure, temperature, and shearing stress in hydrostatic and hydrodynamic bearings. In **Fig. 2**, the results for 2000 rpm are presented, and in **Fig. 3** the results for 4000 rpm are shown. The differences between both types of bearings are the result of different principles of operation, and these differences are very distinct. Film pressure distribution in a hydrostatic bearing shows that, in the area of the pocket, the pressure is constant and equal to the feeding pressure, and outside of the pocket it decreases linearly, accordingly to the theory for pressure losses in a parallel gap. In the hydrodynamic bearing, film pressure is the effect of hydrodynamic phenomena and the distribution is parabolic, as in the relatively small bearing, there is no observable effect of pad deformations. The third set of graphs shows shear stress in the film, also in this case, the differences between two bearings are distinct – in a hydrostatic bearing in the area of the pocket, where the film is very thick shearing stress is small, or even negative due to oil flow irregularities. Much bigger values of shear stress can be observed in the area outside the pocket, where the film is thin. The shear stress distribution to some extent reflects the temperature in the film, which

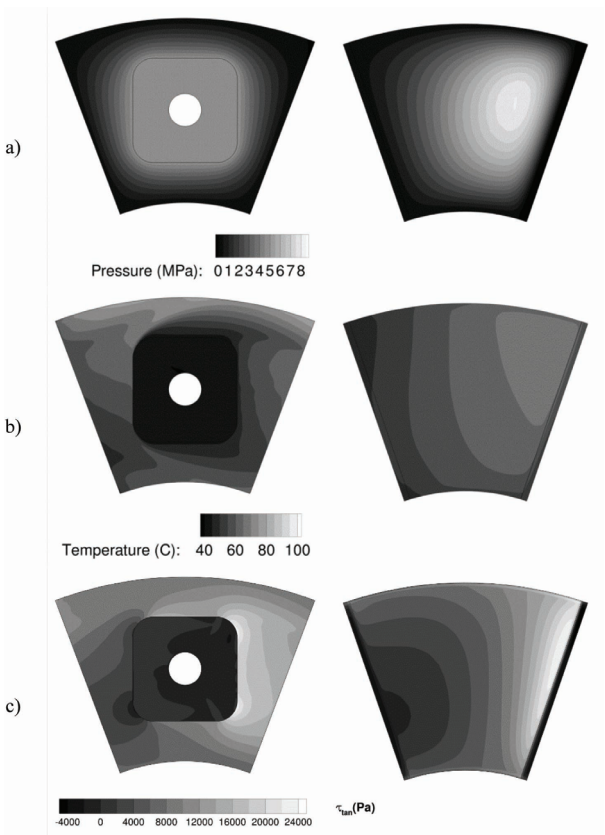


Fig. 2. The contours of pressure (a), temperature (b), and tangential shear stress (c) for hydrostatic (left column) and hydrodynamic (right column) bearing at 2000 rpm (clockwise collar rotation)

Rys. 2. Warstwice ciśnienia w filmie (a), temperatury (b) i naprężeń ścinających w łożysku hydrostatycznym (lewa kolumna) i w hydrodynamicznym (prawa kolumna) dla 2000 obr./min (obrót zgodnie z kierunkiem ruchu wskazówek zegara)

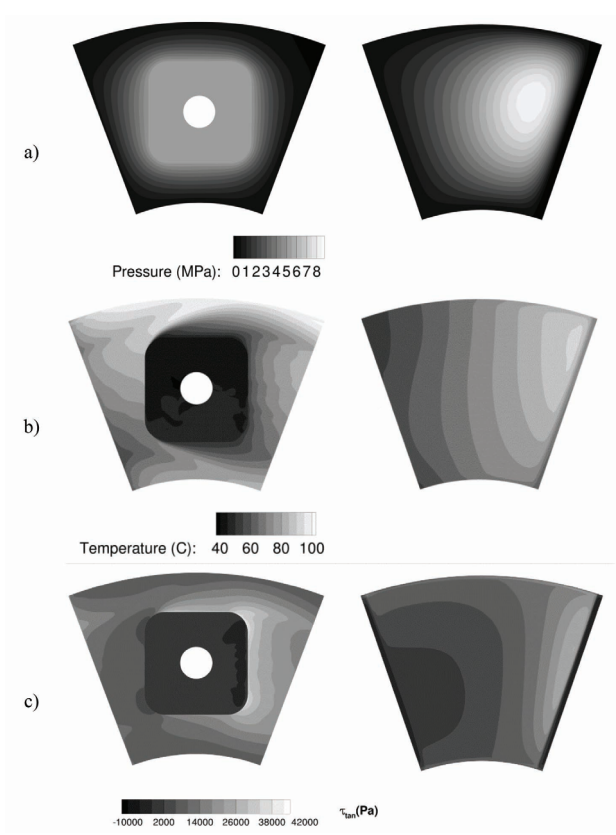


Fig. 3. The contours of pressure (a), temperature (b), and tangential shear stress (c) for hydrostatic (left column) and hydrodynamic (right column) bearing at 4000 rpm (clockwise collar rotation)

Rys. 3. Warstwice ciśnienia w filmie (a), temperatury (b) i naprężeń ścinających w łożysku hydrostatycznym (lewa kolumna) i w hydrodynamicznym (prawa kolumna) dla 4000 obr./min (obrót zgodnie z kierunkiem ruchu wskazówek zegara)

has an influence on oil viscosity – in the areas of lower temperatures, e.g., downstream from the pocket, it has the highest values. In a hydrodynamic bearing, the shear stress distribution is the result of film thickness with increased shear stress in the areas of thinner film. Areas of higher linear velocity situated close to the outer radius are also the areas of higher shear stress. These two effects are changed slightly by decreased viscosity in the areas of higher temperature, e.g., the area close to outer radius and close to the outlet, or increased viscosity in the areas of low temperature, e.g., close to the inner radius.

A very similar distribution of parameters can be observed in the results obtained for 4000 rpm shown in **Fig. 3**. The main difference is that, in the results for 4000 rpm, the effects of temperature and viscosity are more pronounced: Temperature increase in the film is greater, and the influence of cold oil flow from the pocket on the film temperature downstream of the

pocket is larger. The pattern of oil flow from the pocket to the thinner film outside the pocket, both downstream and to the outer and inner radii, can be observed.

Contour plots show the distribution of presented parameters over the surface of the whole pad; thus giving the possibility for qualitative comparison of parameters in both bearings, but it is not easy to compare the parameters quantitatively. That is why a set of graphs presenting selected parameters in selected cross sections was also prepared. Circumferential cross sections at the mean radius and radial cross sections through the middle of the pad, as shown in **Fig. 4**, were selected.

Circumferential pressure and temperature profiles for both bearings are shown in **Fig. 5**, while radial profiles are presented in **Fig. 6**. Pressure distributions are characteristic for both types of bearings; and, since the axial load of the bearing is the same for both speed cases, they are fairly independent from rotational speed. However, the effect of pressure build up before the end of

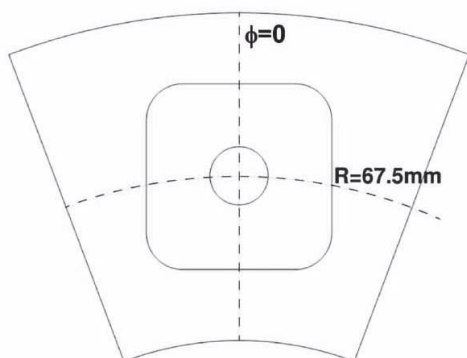


Fig. 4. Schematics of cutting surfaces for Fig. 5 and Fig. 6
 Rys. 4. Schemat płaszczyzn przekroju dla wykresów z Rys. 5 i Rys. 6

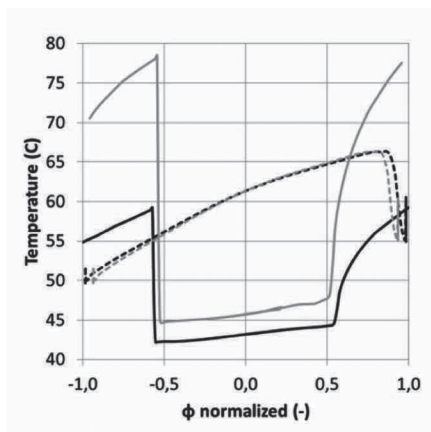
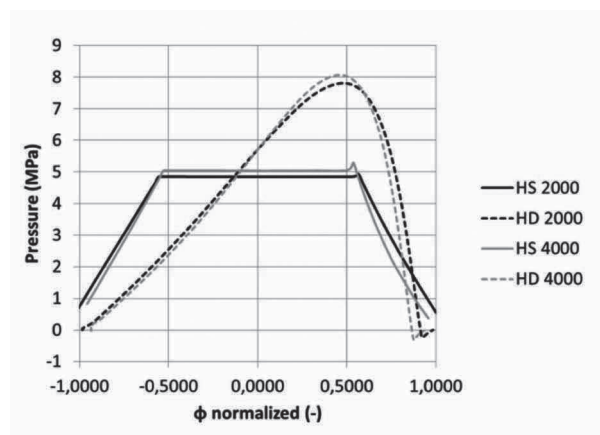


Fig. 5. Pressure and temperature of the bearing pad at 67.5 mm radius for hydrostatic (HS) and hydrodynamic (HD) bearings

Rys. 5. Przebieg ciśnienia w filmie i temperatury w obwodowym przekroju dla promienia 67,5 mm w łożysku hydrostatycznym (HS) i hydrodynamicznym (HD)

the pocket is larger at 4000 rpm. As to the temperatures, one can see that, in the results for 2000 rpm, the hydrodynamic bearing seems to be cooler, while at 4000 rpm, the trend is opposite.

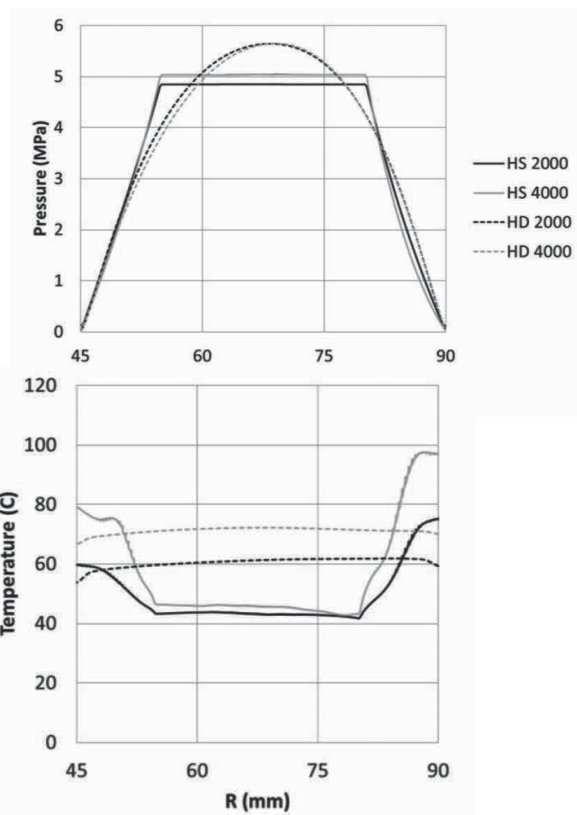


Fig. 6. Pressure and temperature of the bearing pad at angle 00 (middle of the pad) for hydrostatic (HS) and hydrodynamic (HD) bearings.

Rys. 6. Przebieg ciśnienia w filmie i temperatury w promieniowym przekroju dla kąta 0 w łożysku hydrostatycznym (HS) i hydrodynamicznym (HD)

Losses in the bearings

There are various components of losses in the hydrostatic and hydrodynamic bearings – friction losses in the film and losses caused by pumping of the oil. Due to high pressure and considerable oil flow, this component has to be considered in the hydrostatic bearing, while in a hydrodynamic bearing, which does not require the pumping of oil with high pressure, it can be neglected. Friction losses in the film were calculated for both models by integrating the rotational shear stresses on the surface of the pad. Pumping losses are simply the product of volumetric flow rate and the pressure at the inlet.

Table 4. Comparison of losses in both bearings

Tabela 4. Porównanie strat w obu łożyskach

	Hydrostatic (HS)		Hydrodynamic (HD)	
Rotational velocity [rpm]	2000	4000	2000	4000
Friction losses [W]	2033	5911	2280	5372
Pumping losses [W]	324	490	0	0
Total [W]	2357	6401	2280	5371

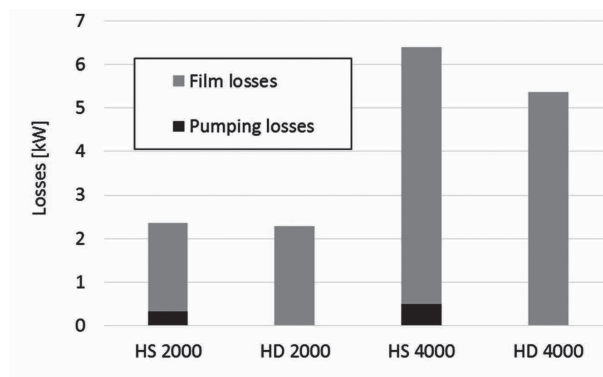


Fig. 7. Comparison of losses in both types of bearings at 2000 rpm and 4000 rpm

Fig. 7. Porównanie strat w obu typach łożysk przy prędkości obrotowej 2000 obr./min i 4000 obr./min

DISCUSSION OF RESULTS AND CONCLUSIONS

It is not possible to compare two bearings with full similarity, because of different principles of operation; however, in this paper, the comparison was done with a realistic technical assumption that both bearings have to carry the same axial load and use the same oil. It was also decided to perform the calculations at approximately the same average film thickness, which

results in much better safety of a hydrostatic bearing, because its minimum film thickness is larger (constant, approximately 30 μm for HS and minimum 9 μm for HD).

The results show that, at the assumed conditions, there was not any decrease of total power losses in the hydrostatic bearing – at a lower rotational speed of 2000 rpm the difference was very small, approximately 3%, but at 4000 rpm, the power losses in a hydrostatic bearing were almost 20% larger than in a hydrodynamic bearing.

Because of thicker film, the hydrostatic bearing can be considered safer (about 30 μm , constant for hydrostatic and minimal 9 μm for hydrodynamic), but the main aim of the study was to find a solution with higher energy efficiency.

Looking at the results, it can be concluded that further study is possible and it should be directed into minimizing film shearing, because this is the substantial component which should be decreased, even at the cost of increased pumping loss, as this component remains much lower. Shearing in the film may be reduced by means of oil viscosity decrease or temperature increase and also by modification of hydrostatic pocket size, since it seems that the basic literature result of optimum pocket size is not valid for a pad thrust bearing with a rotating collar.

REFERENCES

1. Wasilczuk M.: Friction and Lubrication of Large Tilting-Pad Thrust Bearings. *Lubricants* **2015**, 3, 164–180; doi:10.3390/lubricants3020164.
2. Abramovitz S.: Using Hydrostatic Bearings as “Lifts” in Hydroturbines. *Hydro Rev.* 2000, 19, pp. 38–47.
3. Dąbrowski L., Wasilczuk M.: Hydrostatic lift used in a steady state operation of a water turbine thrust bearing, *Nordtrib* 2006.
4. Ettles C.M.M., Seyler J., Bottenschein M.: Some effects of start-up and shut-down on thrust bearing assemblies in hydro-generators. *Transactions of the ASME, Journal of Tribology*, Vol. 125 (2003), p. 824–832.
5. Wasilczuk M.: Wielkogabarytowe hydrodynamiczne łożyska wzdłużne – (Large hydrodynamic thrust bearings – in Polish); Wydawnictwo ITeE: Radom, Poland, 2012, p. 151.
6. Rippel H.: Projektowanie gidrostatycznych podszypników (Design of hydrostatic bearings – in Russian translated from English). *Izdatelstwo Maszynostrojenie*, Moscow, Soviet Union, 1967, p. 16.
7. Dąbrowski L.; Wasilczuk M.: Influence of hydrostatic pump operation period on performance of a thrust bearing of a 125 MW pump-turbine. *Mecanique Ind.* 2004, 5, 3–9.
8. Wasilczuk M., Wodtke M., Braun W.: Centrally Pivoted Tilting Pad Thrust Bearing with Carbon-Based Coated Collar—Experimental Results of Low- and Medium-Speed Operation. *Tribology Transactions*, vol. 58 (nr 5), 2015, s. 882–893.
9. Menter F.R., Two-Equation Eddy-Viscosity Turbulence Models for Engineering Applications. *AIAA Journal*. 32(8). 1598–1605. August 1994.
10. Wodtke M., Olszewski A., Wasilczuk M.: Application of the fluid-structure interaction technique for the analysis of hydrodynamic lubrication problems. *Proc IMechE, Part J: Journal of Engineering Tribology*, 2013, vol. 227 (8), s. 888–897.